ADVANCED FUNCTIONAL MATERIALS
www.afm-journal.de

An Edible Supercapacitor Based on Zwitterionic Soy Sauce-Based Gel Electrolyte

*Mete Batuhan Durukan, Deniz Keskin, Yiğithan Tufan, Orcun Dincer, Melih Ogeday Cicek, Bayram Yildiz, Simge Çınar Aygün, Batur Ercan, and Husnu Emrah Unalan**

With rapid technological developments, the use and reliance on small and miniaturized electronics have increased significantly. Prevalent power sources used in wearable and implantable devices are based on potentially toxic materials. This creates massive environmental problems and generates waste that requires novel and sustainable solutions in the Internet of Things era. Alongside newly developed biodegradable and implantable devices, edible and ingestible electronic devices have emerged to create a niche and sustainable solution. To realize these devices, energy sources must also be edible and ingestible. Here, zwitterionic and edible gel electrolytes are produced using hydroxyethyl cellulose and commercial soy sauce (shoyu) for superior ionic conductivity, providing a favorable environment for L929 proliferation. These edible gels are combined with carbon electrodes to fabricate edible supercapacitor devices, resulting in an ideal double-layer capacitance. These gels have been discovered to operate at sub-zero temperatures and possess anti-drying properties. Introducing an edible soy sauce-based gel with impressive ionic performance provides a promising alternative to conventional energy storage devices, enabling the advancement of cutting-edge ingestible healthcare devices and environmentally friendly electronics.

1. Introduction

Efforts in healthcare research in the 21st century focused on continuous physiological monitoring via implantable devices and wearable electronics.[1] These would allow in-vivo monitoring with high specificity, opening a new age in the healthcare industry for patient-care and diagnosis.[2–4] Although implantable devices offer an excellent way for in-vivo analysis, they are highly invasive and can cause complications in the patient's body.[1] To overcome this problem, within the framework of the targeted application, it is necessary to develop a new generation of edible electronics classified as innovative, miniaturized, and ingestible medical technology. Ingestible electronics (IE) are eme as a solution, whichcollects data and monitor physiological symptoms simultaneously.[5–9] Examples of this new medical technology range from biosensors to micro and optoelectronic devices.[10,11] In 2011, the United States Food and Drug Administration (FDA) approved the first ingestible digital system as the first futuristic vision of edible electronics.[12] Later, with the development of new biocompatible, green, and biodegradable materials, edible electronic devices evolved as a new concept, enabling new technologies and broadening the horizons of electronics and materials science.[13] Although there are no regulations governing the health criteria of edible electronics, some organizations are developing guidelines for the food and pharmaceutical industries, such as the FDA, the European Food Safety Authority (EFSA), and the European Medicines Agency.[14] A potential

M. B. Durukan, D. Keskin, Y. Tufan, O. Dincer, M. O. Cicek, B. Yildiz, S. Çınar Aygün, B. Ercan, H. E. Unalan
Department of Metallurgical and Materials Engineering
Middle East Technical University (METU)
Ankara 06800, Türkiye
E-mail: unalan@metu.edu.tr

The ORCID identification number(s) for the author(s) of this article can be found under https://doi.org/10.1002/adfm.202307051

DOI: 10.1002/adfm.202307051

M. B. Durukan, S. Çınar Aygün, H. E. Unalan
ENDAM
Energy Storage Materials, Devices Research Center
Middle East Technical University (METU)
Ankara 06800, Türkiye

B. Ercan
Biomedical Engineering Program
Middle East Technical University (METU)
Ankara 06800, Türkiye

B. Ercan
BIOMATEN, Center of Excellence in Biomaterials and Tissue Engineering
Middle East Technical University (METU)
Ankara 06800, Türkiye

approach to evaluate possible interactions following the consumption of ingestible electronics is to investigate the effect of edible electronics on cellular growth, proliferation, and spreading in vitro.[15–19]

One way to power up edible electronics is to use transient, biodegradable, and edible energy storage devices.[9,20–25] Supercapacitors (SCs) are excellent candidates for energy storage in edible electronics due to their long lifetime, high power densities, and simple design.[26] For edible supercapacitors, edible electrolytes' material possibilities are limited to foods or synthetic products derived from foods.[27] To date, few studies have reported electrolytes for edible supercapacitors. While examples of edible liquid electrolytes include Monster energy drink, V8 vegetable drink, Gatorade drink, and agar aqueous solution, only a few studies utilized gel electrolytes, including sodium chloride (NaCl) enriched agarose, dough gel, and soy protein isolate gel.[28–35] Zwitterions are a famous type of molecule having both anionic and cationic counterparts in their monomeric formula and can be an alternative to the electrolytes mentioned above.[36,37]

Zwitterions retain water and boost ionic conductivity by forming ion migration channels.[38] Taking advantage of this functional feature of zwitterions, Peng et al. demonstrated how zwitterionic gel electrolytes improve the electrochemical performance of supercapacitors. When an electric field is applied, the zwitterionic groups align, and ion migration channels are created in zwitterionic electrolytes, improving the overall performance of the electrolytes.[39] Ion migration channels improve ion transport, allowing easy separation of positive and negative ions in the electrolyte. Electrostatic interactions between ions and charged groups are, then, easily overcome, and the separated ions are rapidly transferred to the electrode surfaces. Thus, the capacitance and rate capability of supercapacitors are greatly enhanced.[40] Zwitterionic gel electrolytes can also retain a significant amount of water due to strong interactions between charged groups and water molecules. For instance, Liu et al. compared the water retention ability of zwitterionic PAA-co-PDP hydrogel with that of the PAM hydrogel. While the zwitterionic PAA-co-PDP hydrogel retained its shape with only 34% loss of water content after 72 h, the PAM hydrogel could not retain its shape with a significant loss of water content (82%), indicating the superior water retention ability of zwitterionic structures.[41]

It is clear that the development of zwitterionic monomers opens a chapter in the design of next-generation electrolytes. However, current studies on zwitterionic gel electrolytes only focus on the design of zwitterionic polymers using different moieties. The design process is expensive, time-consuming, and impractical. Moreover, the use of many chemical reagents and potentially harmful chemicals is detrimental to the environment. Proteins, on the other hand, are harmless to the environment, and it has been proven that they have conductance at a molecular level, especially in the hydrated state.[42,43] More interestingly, proteins – especially soybean protein isolates – were also used to improve the performance and stability of the electrolyte for energy storage devices.[44,45] Inspired by these, in this work, we propose a zwitterionic, anti-freezing, and anti-drying edible gel electrolyte with high ionic conductivity of 1.3×10^{-1} S cm^{-1}, using only food-based materials. A food-based material, commercial soy sauce, is used for the ionic conductivity, while hydroxyethyl cellulose (HEC) is used as the polymer backbone. To facilitate excellent conductivity, the zwitterionic nature of amino acids in soy sauce is exploited by changing the pH conditions using acidity regulators commonly found in food products. L929 fibroblasts are exposed to gel-dissolved cell culture media to prove the cytocompatibility of the fabricated gels in vitro. Fabricated zwitterionic gel electrolytes are combined with carbonaceous electrodes prepared using HEC, glycerol, carbon black (CB), and activated carbon (AC). Edible supercapacitors utilizing edible soy sauce-based electrolyte (E-SGE) and HEC:glycerol:CB:AC (HGC) electrodes resulted in a specific capacitance of 3.75 F g^{-1} at a scan rate of 30 mV s^{-1}. Excellent cycling stability with a capacitive retention of 86.5% is obtained after 10 000 cycles. Due to the superior kinetics and conductivity offered by the zwitterionic properties of soy protein, fabricated edible supercapacitors can be used at a scan rate of 3 V s^{-1} and can be used at temperatures as low as −24°C without significant loss of performance. Edible supercapacitors can be stored for long periods at sub-zero temperatures and used on demand without significant loss in performance. Lastly, the digestibility of edible supercapacitors is investigated in simulated gastric fluid, showing that digestion occurs within one hour.

2. Results and Discussion

Figure 1 schematically shows the fabricated supercapacitor device's edible and zwitterionic soy sauce gel electrolyte (E-SGE) configuration with a typical zwitterionic amino acid provided by the rich protein content of the soy sauce. A combination of gelatin, glycerol, HEC, and soy sauce is used to fabricate E-SGEs, while the combination of glycerol, HEC, and carbon mixture is used to fabricate HGC electrodes. By using edible components, the final structure of the supercapacitor reaches its edible form.

The protein structure in the E-SGE matrix ultimately has zwitterionic amino acids at the molecular level. Typically, E-SGE is made of HEC as a polymer matrix and soy sauce as a solvent. Soy sauce (shoyu, to be exact) is an easily accessible and commercialized condiment used in almost every country. It is rich in essential nutrients ranging from proteins to vitamins. Besides its high nutritional value, soy sauce has a high salt content ranging from 14% to 19% (w/v). The salt (NaCl) molecules dissolve into their component ions in aqueous media, sodium (Na^+), and chloride (Cl^-), giving more free ions into the electrolyte. Soy sauce is not only rich in sodium (Na^+) and chloride (Cl^-) ions, but it also has calcium (Ca^{+2}), sulfates (SO_4^{-2}), and phosphates (PO_4^{-3}), which then again help to improve its electrochemical performance. The electrolytes that have high salt content are called "polymer-in-salt electrolytes."[46] High salt concentration in "polymer-in-salt electrolytes" acts as a plasticizer of the polymer network, leading to extremely high ionic conductivity. Although a plasticizing effect is desired for conductivity, it adversely affects mechanical properties.[47]

In the investigated E-SGE, HEC is used as the matrix to obtain a gel electrolyte. Being highly biodegradable and biocompatible, HEC is an ideal material for the E-SGE.[48] HEC is an edible cellulose derivative biopolymer that can provide prominent ionic conductivity due to its massive number of hydroxyl (-OH) groups.[49–57] Furthermore, hydroxyl groups (-OH) interact with polar groups such as amine groups ($-NH_3^+$) and carboxyl groups (-COOH) on proteins in soy sauce resulting in

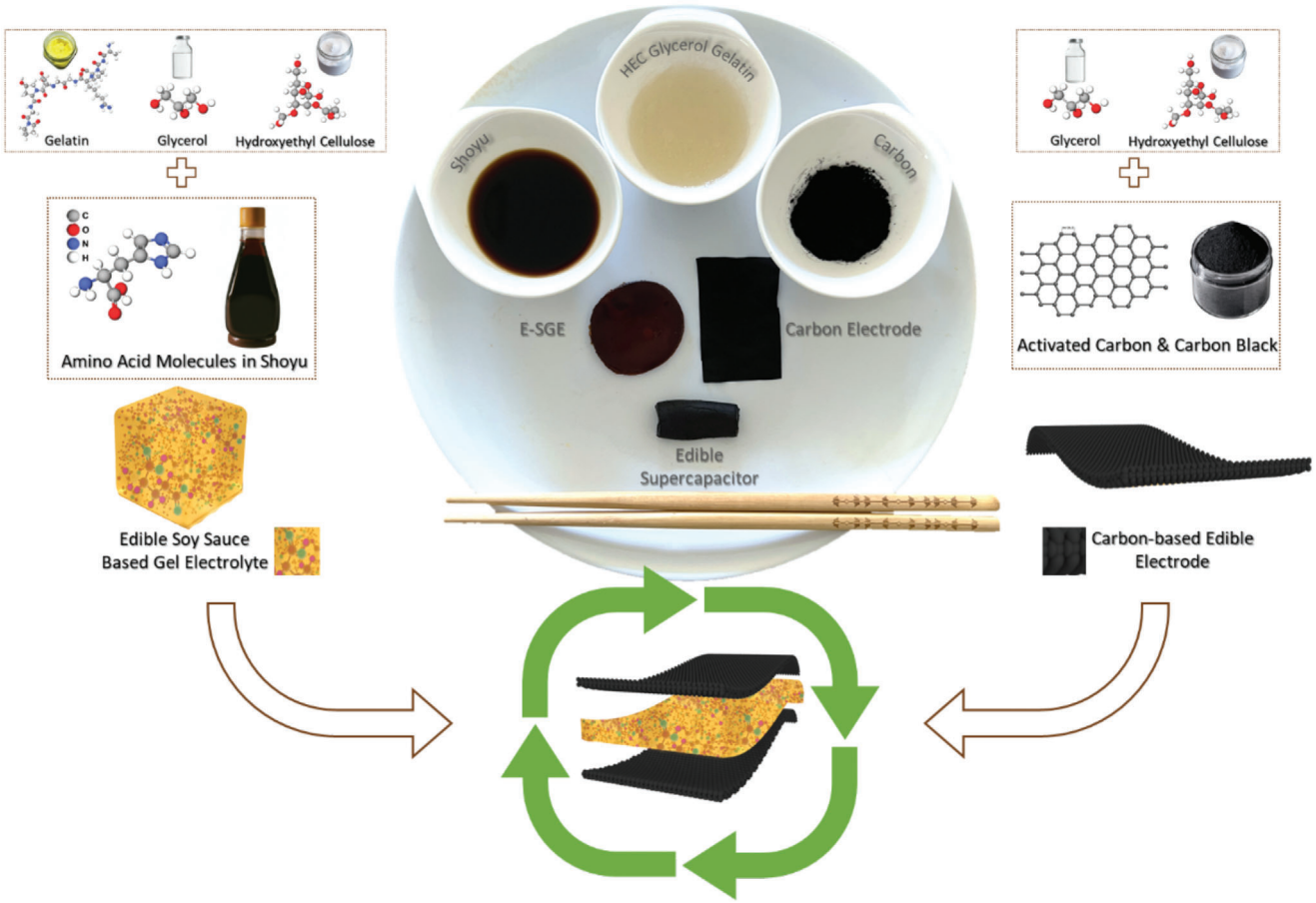

Figure 1. Schematic illustration and photographs of materials used for the fabrication of edible supercapacitors.

cross-linked structure.[58] To further increase water retention ability and cycling stability, this work adds edible ingredients such as gelatin and vegetable-origin glycerol to the E-SGE.[59–62] Addition of the gelatin and vegetable-origin glycerol also increased the mechanical stability and improved the gelation. E-SGE can be flexed or twisted without any permanent deformation. This proves that they do not cause problems either by being plasticized with a high amount of salt or by drying in ambient conditions (Figure S1a, Supporting Information). It has also been observed that the E-SGE surface has a uniform micro-roughness (Figure S1b, Supporting Information).

In order to fabricate the supercapacitor, carbon-based electrodes are prepared by simple mixing followed by doctor blading using an HEC matrix. A mixture of CB and AC in the HEC/Glycerol matrix is used as the anode and cathode electrodes (HGC), while the edible E-SGE is utilized as both the electrolyte and separator. AC, also known as activated charcoal, is classified as edible and used in many food products.[4] Carbon black from vegetable origin functions as an additive for food coloring in many European countries.[63] The large surface area of the AC and the high conductivity of CB make this mixture an ideal electrode material for supercapacitors with high electrochemical performance.[64] The fabricated electrodes mechanically behave like a thin foil and can be bent or folded without any mechanical deformation (Figure S1c, Supporting Information). SEM images provided in Figure S1d (Supporting Information) show that the surface of the fabricated carbon-based electrodes is highly porous. HGC electrodes had an electrical resistance of 40 Ω sq^{-1} with an average thickness of 10 μm, allowing HGC electrodes to be used without additional conductive substrates. This enabled the utilization of E-SGE within a completely edible supercapacitor. Edible supercapacitors are obtained by combining these HGC electrodes with E-SGE. With the combination of flexible electrodes and the electrolyte, fabricated edible supercapacitors can be flexed and even rolled smoothly (Figure S1e, Supporting Information).

Soy sauce is made up of mainly fermented soybeans and starch material, in addition to a high salt content. Rich protein content in soy sauce, on the other hand, comes from two different sources – soy proteins and wheat proteins.[65,66] The starch material, such as wheat, rye, and barley used in soy sauce, has a 3D gluten network. This 3D gluten network not only overcomes the drawbacks of the plasticizing effect of high salt content, but also helps to improve ionic conductivity by forming ion transport pathways with its porous nature.[67] Last but not least is the rich protein content that soy offers, which makes up ≈20% of its total weight.[66,68] Enzymes in naturally brewed soy sauce convert some of these proteins into their monomeric forms, amino acids.[69] Examples of amino acids in soy sauce include glutamic acid, aspartic acid, leucine, histidine, alanine, arginine, lysine,

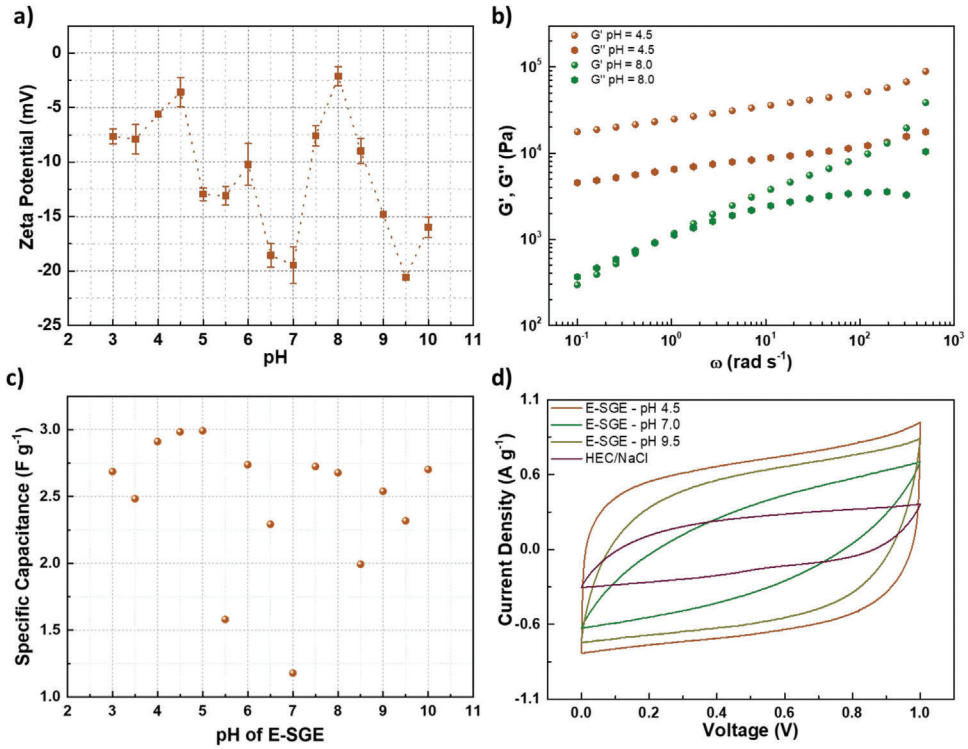

Figure 2. a) Zeta potential plot for E-SGEs as a function of pH. b) Storage modulus and loss modulus as a function of angular frequency for the determination of gel-like structure. c) Specific capacitance values as a function of pH at a scan rate of 200 mV s^{-1}. d) Cyclic voltammogram comparisons of the best-performing E-SGE compared to the ones with the lowest surface charge values and a typical HEC/NaCl electrolyte.

valine, tyrosine, glycine, tryptophan, serine, proline, methionine, isoleucine, threonine, etc.[70,71]All amino acids have a simple and similar structure that is a chiral carbon center with different side groups specific to that amino acid. While some amino acids in soy sauce are polar, such as glutamic acid and arginine, some are nonpolar, such as alanine and leucine. Some amino acids, such as histidine, have ionizable charged groups in their side chain.[72] Despite having different properties defined by the structure of their side chains, all amino acids have a typical zwitterionic structure with an amine group (-NH_2) and a carboxyl group (-COOH). Near their isoelectric point, the amine group accepts a proton (H^+) to turn into an ammonium cation (-NH_3^+), whereas a strong proton donor carboxyl group gives hydrogen (H^+) cation to form a carboxylate anion (-COO^-). These together form zwitterionic amino acids with a net charge equal to zero.[73] This is typically achieved by adjusting the pH of the medium, as the zwitterionic compounds are prone to protonation or deprotonation.

Understanding the surface charge of the soy sauce is essential to determine the pH corresponding to the isoelectric point. To prove the above-mentioned zwitterionic behavior of E-SGE, zeta potential measurements are performed with electrochemical measurements on soy sauce used in the fabrication of electrolytes. When the pH is adjusted closest to the isoelectric point (pI), i.e., pH corresponding to the lowest solubility, the molecule has the highest ionic conductivity thanks to the charged groups, as mentioned earlier. At pH values below the isoelectric point, zeta potentials are expected to be positive due to the protonation mechanism of amino acids. The dominant deprotonation mechanism in the carboxylate group (-COO-) results in negative zeta potential values at higher pH values. In this case, an anionic behavior is observed from pH 3 to 11, provided in **Figure 2**a. This phenomenon may be due to presence of amino acid groups, namely aspartic acid, glutamic acid, histidine, and lysine in soy protein. It is possible to theoretically calculate the expected charges by using the Henderson – Hasselbach equation depending on these four amino acids, which are reported to have a net negative charge in the acidic region.[74] Also, this may be due to the adsorption of chloride (Cl^-) ions from the salt content in commercial soy sauce.[75]

In this completely anionic behavior, pH 4.5 and pH 8 are the closest points to the pI. The pI, at a pH of 4.5, is attributed to soy proteins in soy sauce, which has an isoelectric point in the range of 4.0 to 5.0.[76–79] The second isoelectric point is observed at a pH of 8, which is unexpected. This is probably related to the presence of gluten in the soy sauce, as gluten has an isoelectric point between 6.0 and 8.0.[80,81] When pH gets closer to 8, the agglomeration of gluten molecules causes poor cross-linking and poor hydration.[82,83] As a result, E-SGE fabricated at a pH of 8.0 does not have a gel-like structure. Rheological measurements are conducted to observe the differences in mechanical properties of the E-SGE at pH values of 4.5 and 8.0 (Figure 2b). The measurements provided the storage modulus, G', and loss modulus, G'', with respect to applied angular frequency. E-SGE prepared at a pH of 4.5 shows a good example of a physical hydrogel, where $G' \gg G''$ at all frequencies.[84,85] This is due to the solid-like properties of the E-SGEs, which are already shown in Figure 2b. On the other hand, E-SGEs prepared at a pH of 8.0 show a viscoelastic liquid with $G' \gg G''$ at high frequencies yet $G' < G''$ at low

frequencies.[85] This confirms the excellent zwitterionic behavior of soy proteins at pI, attributed to the high hydration capacity provided by the strong interactions between the charged groups and water molecules.[36]

The performance enhancement of E-SGEs originating from the zwitterionic state is verified using cyclic voltammetry (CV) and potentiostatic impedance spectroscopy (PEIS). Supercapacitor devices formed with E-SGEs prepared at different pH values are compared to determine the best-behaving electrolyte. Detailed cyclic voltammograms taken at a scan rate of 200 mV s^{-1} and impedance analysis results comparing the effect of pH values are given in Figure S2 (Supporting Information). In the initial observation from the cyclic voltammograms in Figure S2a,b (Supporting Information), it is observable that most of the E-SGEs work quite well in terms of ideal EDLC behavior. The best capacitance values are obtained at pH 4.5 and pH 5.0, but most samples below -15 mV zeta potential perform quite well in terms of performance (Figure 2c). This may be due to the presence of zwitterionic molecules even though the net charges are not zero. The correlation is especially hard due to the structure of soy protein – where some charged groups may reside in the protein core[74], which becomes particularly complex in a commercial soy sauce. Nevertheless, a general performance increase can be deduced by the increase in zwitterionic behavior, which is highly evident in the impedance spectra provided in Figure S2c,d (Supporting Information). The best impedance results with the smallest semicircle are obtained at pH 4.5, which indicates a very high ionic conductivity (Figure S2c, Supporting Information). Although comparable results are obtained at basic pH values, their mechanical instability and the inability to achieve physical hydrogel formation is problematic. Therefore, E-SGEs prepared at pH 4.5 are chosen as the best-performing electrolytes. To further prove the added performance of zwitterionic amino acids, cyclic voltammograms of devices with E-SGE at a pH of 4.5 are compared to those with the least performing electrolyte and a simple HEC/NaCl electrolyte. Devices with HEC/NaCl electrolytes are prepared in the same way without the complex components of soy sauce to compare their performances with E-SGE. Cyclic voltammograms for comparison, at a scan rate of 200 mV s^{-1}, are provided in Figure 2d. As can be seen, the device with E-SGE prepared at pH 4.5 has much higher performance than those devices prepared with mostly charged E-SGEs (pH 7 and pH 9.5). Moreover, E-SGE outperformed the typical HEC/NaCl electrolyte. All of these results proved that the performance of zwitterionic amino acids increases at appropriate pH, which is closely tied to its pI.

FTIR analysis is done on E-SGEs in every step of the fabrication and compared with each other to fully understand the changes in the structure. Related FTIR spectra of HEC, HEC/Soy Sauce, HEC/Soy Sauce/Gelatin, HEC/Soy Sauce/Gelatin/Glycerol (E-SGE), and soy protein isolate are provided in Figure S3 (Supporting Information). Overall, step-by-step addition of every ingredient can be observed with FTIR, with the successful blending that provides a characteristic addition or change in the spectrum. The most important part is the appearance of NH_3^+ and COO^- at pH 4.5, which is attributed to the zwitterionic state of the E-SGEs, which is observed by FTIR measurements (Figure S4, Supporting Information) in liquid form.[86,87] The change in overall behavior is also observed with thermal gravimetric analysis (TGA) and related plots are provided in Figure S5 (Supporting Information). E-SGEs have higher thermal stability with much better water retention capability especially due to the addition of gelatin and glycerol. A detailed description of the interactions between HEC, soy sauce, gelatin, and glycerol via FTIR and TGA is provided in Supporting Information.

Besides the structural characterizations of E-SGEs, it is imperative to closely control the interactions of the decomposed molecules during and after digestion by investigating whether the produced edible gel electrolytes are biocompatible. Accordingly, the cytotoxicity of edible gel electrolytes is assessed using L929 fibroblasts (ISO 10 993). To assess the cytotoxicity of edible gel electrolytes, E-SGEs are dissolved in a cell culture medium in different concentrations. Cells are seeded on tissue culture plates and exposed to gel-dissolved mediums under standard cell culture conditions (37 °C and 5% CO_2). The biological properties of E-SGEs are assessed using L929 fibroblasts. Cells are cultured in media containing 0.5, 1, 2, and 6 g L^{-1} E-SGE for up to five days in vitro. MTT assay results at the designated time points are provided in **Figure 3**a. The cellular proliferation results did not reveal any differences between the cells cultured in E-SGE dissolved and control (no E-SGE) media on the 1st day of culture (p>0.05). However, on the 3rd day in vitro, cellular proliferation differed between the sample groups. Cells cultured in media containing 0.5 g L^{-1} E-SGE expressed higher cellular proliferation than those cultured in media containing 1, 2, and 6 g L^{-1} E-SGE ($p < 0.001$). In addition, cells cultured in 6 g L^{-1} E-SGE dissolved media had slightly less cellular proliferation than those cultured in 2 g L^{-1} E-SGE ($p < 0.01$). On the 5th day of culture, the differences observed in cellular proliferation on the 3rd day diminished. However, cellular proliferation is still the highest for the control group compared to those cultured in E-SGE dissolved media ($p < 0.001$). It is important to note that fibroblasts proliferated for up to 5 days independent of the E-SGE concentration inside the culture media. To better understand the effect of E-SGEs on cellular behavior, cell morphologies are characterized on the 3rd day of culture. SEM images of cells exposed to the standard medium (control) and the E-SGE dissolved medium (6 g L^{-1}) are shown in Figure 3b. SEM images revealed that fibroblasts cultured in 6 g L^{-1} E-SGE dissolved medium spread better than the control samples. This observation is further confirmed with confocal microscopy (Figure 3c). Cellular spreading is quantified, and the results are provided in Figure 3d. The average spreading of fibroblasts cultured in regular medium and 6 g L^{-1} E-SGE dissolved medium is calculated as 865 ± 220 and 1422 ± 309 μm^2 per cell, respectively. These biological findings are consistent with the literature. Several studies showed that soy protein enhances fibroblast functions.[88,89] For instance, Tokudome et al. observed that adding soybean peptide to the culture medium improved collagen synthesis of the fibroblasts.[90] In another study, fibroblast proliferation, migration, and functions cultured on scaffolds are accelerated by incorporating soy protein.[91] These findings are explained by the increased expression of the extracellular signal-regulated kinase (ERK) and integrin $\beta 1$ in fibroblasts in the presence of soy protein, where ERK is reported to regulate actin organization and cell motility, and integrin $\beta 1$ is known to regulate cell migration and the production of new extracellular matrix proteins.[92,93] In this study, E-SGEs in the cell

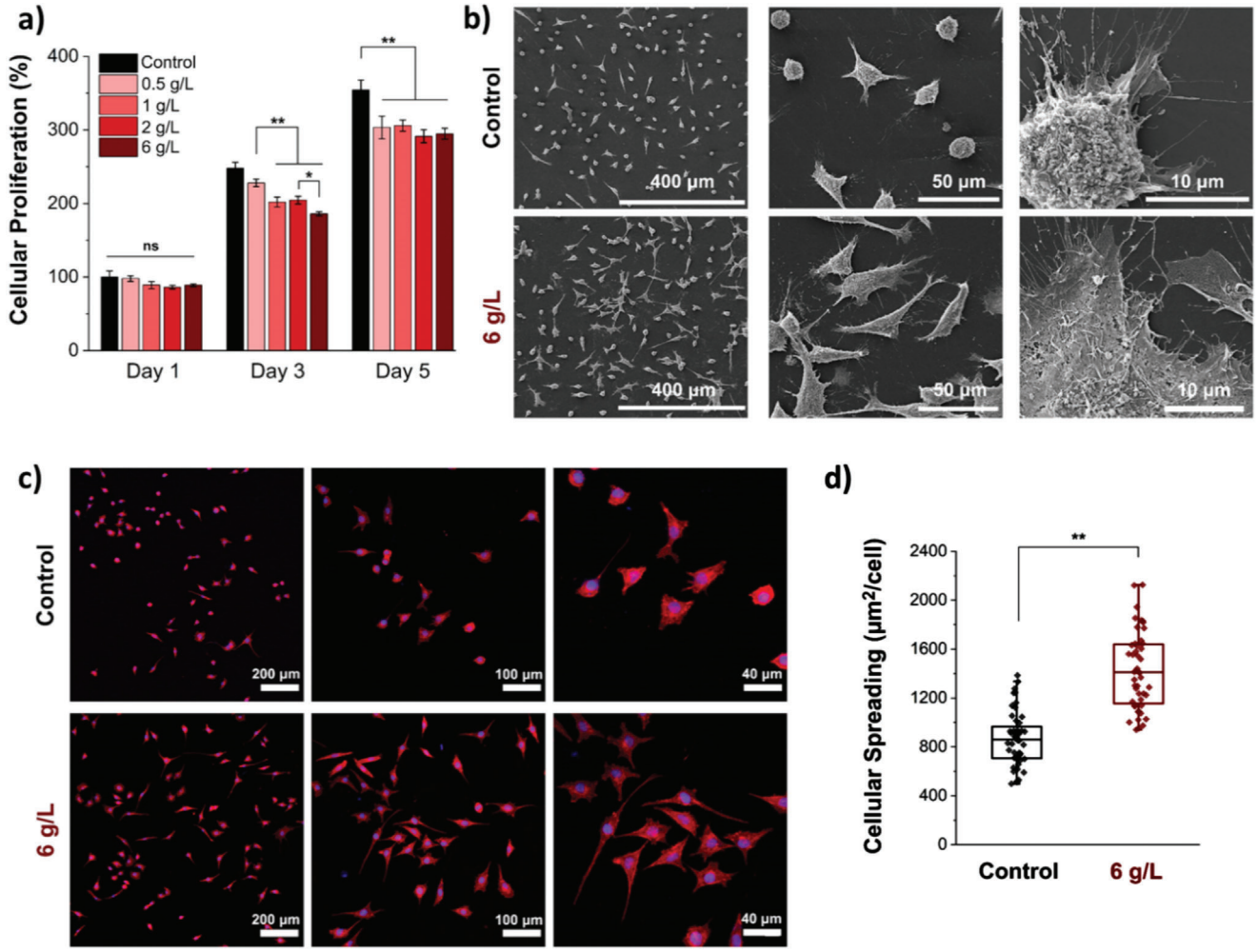

Figure 3. Biological characterizations of the E-SGEs. a) MTT assay results of L929 fibroblasts cultured in media containing 0.5, 1, 2, and 6 g L^{-1} E-SGE. b) SEM images, c) confocal microscopy images, and d) cellular spreading of the cells exposed to the standard culture medium (control) and media containing 6 g L^{-1} E-SGE on the 3rd day in vitro. *$p < 0.01$, **$p < 0.001$, ns: non-significant.

culture medium might have enhanced fibroblast spreading by supplying additional essential amino acids (such as lysine, leucine, histidine) to the cells and increasing the protein and carbohydrate content of the culture medium.[94] Collectively, E-SGEs supported cellular proliferation and enhanced cellular spreading in vitro. These results show that the prepared E-SGEs are not harmful and even support cellular growth. The cytotoxicity results can be correlated with the possible edibility and digestibility of E-SGEs, further suggesting that E-SGEs can be used in various applications requiring biocompatibility.[95]

Edible supercapacitors formed with E-SGEs fabricated at pH 4.5 are subjected to comprehensive electrochemical analysis, and the results are provided in **Figure 4**. Cyclic voltammograms (CVs) are obtained within a voltage range of 0 and 1.0 V at scan rates ranging from 30 mV s^{-1} to 3 V s^{-1} (Figure 4a,b). Zwitterionic presence due to soy proteins in E-SGEs resulted in an almost perfect EDLC behavior. This is evident as the typical rectangular shape is conserved upon increasing the scan rate from 30 mV s^{-1} to 3 V s^{-1}. Gravimetric capacitances are calculated from these CVs, and provided with respect to the logarithmic scan rate in Figure S6 (Supporting Information). A maximum specific capacitance of 3.75 F g^{-1} is obtained at a scan rate of 30 mV s^{-1}, which behaves linearly with the logarithmic scale of scan rates. This indicates an ideal supercapacitive behavior, as suggested by the CV shapes. The PEIS results in Figure 4c confirm this ideal behavior. Insets show the equivalent circuit model and the high-frequency region. The low series resistance of 3.4 Ω (R_1), which can be seen in the inset graph, is a result of the high conductivity of the carbon-based electrodes. The small semicircle, ≈1.1 Ω (R_2) in diameter, suggested minimal interfacial resistance, indicating good adhesion between the HGC electrodes and E-SGEs. Here, the presence of a constant phase element (CPE – Q_2) results from ionic migration between the electrodes and electrolyte layer. Low-frequency region has almost an ideal slope – which again constitutes a CPE (Q_3) due to the deviation from a theoretical double-layer capacitance. This is expected as E-SGEs are solid-like gels with ionic characteristics. Nevertheless, the dimensionless CPE exponent from the proposed equivalent circuit is found to be 0.8783. This is very close to 1, where the supercapacitor would behave completely as an ideal capacitor, further

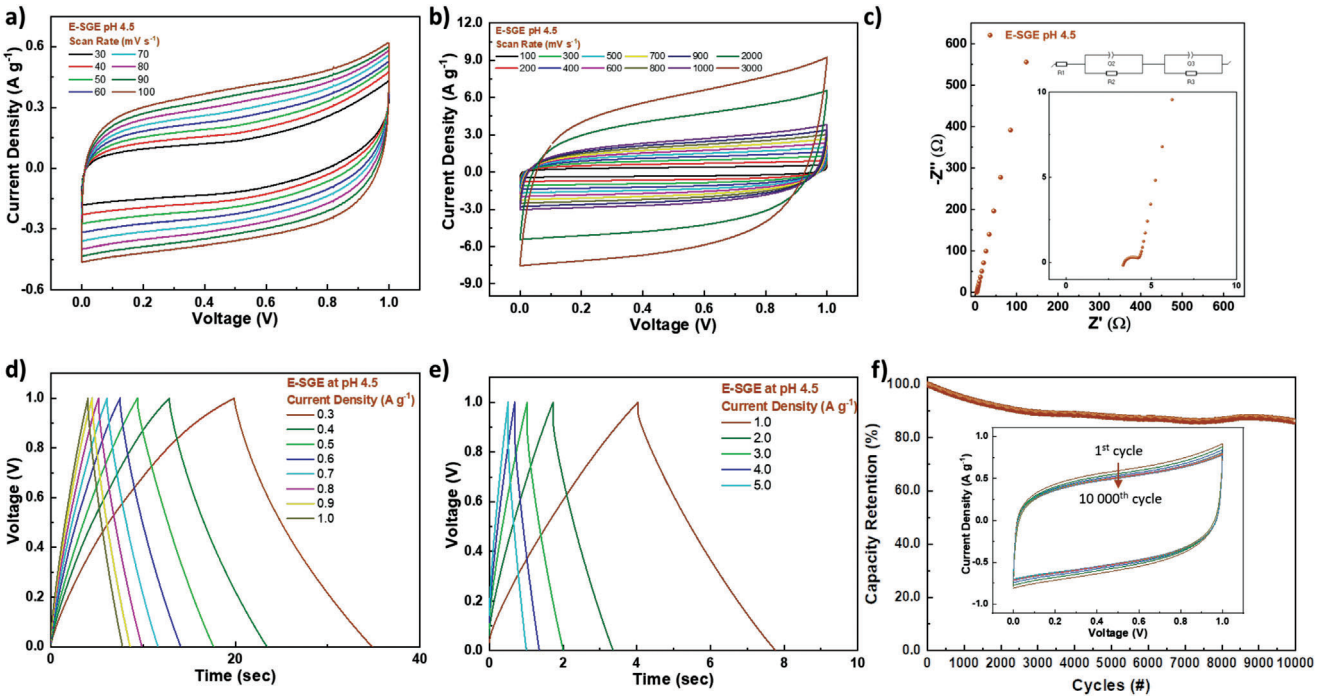

Figure 4. Thorough electrochemical analysis of edible supercapacitors utilizing E-SGEs prepared at a pH of 4.5. CVs at a) low and b) high scan rates. c) Impedance spectra of the edible supercapacitors. The inset graph shows the high-frequency region, while the inset circuit is the equivalent circuit for the obtained Nyquist spectra. Galvanostatic charge-discharge measurements at d) low and e) high current densities. f) Capacity retention results from the repeated cyclic voltammetry for 10 000 cycles at a scan rate of 200 mV s^{-1}. The inset graph shows the results of the CV measurement taken every 1000 cycles.

indicating the promising performance of E-SGEs.[96] The ionic conductivity of E-SGEs is also calculated from PEIS and is found as 1.3×10^{-1} S cm^{-1}, one of the highest values ever reported in the literature.[8,97] Further electrochemical characterization is conducted through galvanostatic charge-discharge (GCD) measurements. GCD measurements are conducted at current densities ranging from 0.3 to 5 A g^{-1}, the results of which are provided in Figure 4d,e. Almost triangular shapes show that the edible supercapacitors work ideally with a very low IR drop, even at high current densities. Energy and power density values are calculated using GCD curves and the results are plotted on a Ragone plot given in Figure S7 (Supporting Information). A maximum energy density and power density of 0.62 W h kg^{-1} and 2500 W kg^{-1} are obtained from the current densities of 0.3 A g^{-1} and 5 A g^{-1}, respectively. The capacity retention of the edible supercapacitors is also investigated by repeating CV measurements for 10 000 cycles (Figure 4f). A retention rate of 86.5% is obtained at the end of 10 000 cycles, showing significant stability of the edible supercapacitors. The inset graph in Figure 4f also shows that the ideal supercapacitive behavior is retained during these 10 000 cycles. All in all, edible supercapacitors fabricated by utilizing E-SGEs show promising electrochemical results. These results showed that soy sauce, a well-known condiment, can be utilized as an electrolyte ingredient to fabricate high-performance edible energy storage devices.

Flexibility is also an important aspect of supercapacitor applications. Hydrogel properties of E-SGEs are demonstrated in Figure 2b, and the flexibility of carbon-based electrodes (Figure S1c, Supporting Information) played a crucial role in enabling flexibility in the fabricated edible supercapacitors. This is explored by CV measurements taken under different flexing conditions. Cyclic voltammograms and photographs attributed to the measurements are given in Figure S8 (Supporting Information). The folded sample displayed exceptional flexibility as an edible supercapacitor, with a maximum capacitance loss of 16%.

Anti-drying and anti-freezing properties are essential for the operation of an edible supercapacitor.[97,98] However, no studies have focused on the development of these capabilities for edible devices, including supercapacitors. E-SGEs made from soy sauce as a protein-rich food product can take advantage of protein content and its zwitterionic structure. Thanks to the synergistic effect of zwitterionic amino acids, high salt content, and gelatin, anti-drying properties and freezing tolerance are enhanced. In addition, glycerol added to the E-SGEs forms abundant hydrogen bonds with water. These bonds prevent the formation of ice crystals and the evaporation of water.[99] TGA results provided in Figure S4 (Supporting Information) have already proven that E-SGEs improve water retention. Photographs provided in Figure S9a,b (Supporting Information) show physical changes in a standard HEC/NaCl and E-SGE kept under ambient conditions (+25 °C with 25% moisture) for 5 days. Dimensional changes are recorded to monitor the anti-drying properties of both electrolytes. HEC/NaCl electrolyte starts shrinking immediately after 2 days, with an ultimate dimensional loss of 45% after 5 days. E-SGE, on the other hand, shows a dimensional loss of only 5% after 5 days. This evidence demonstrates that incorporating zwitterionic proteins derived from soy sauce enhances resistance to drying and verifies the presence of their water retention

properties through the negligible degree of shrinkage observed under normal environmental conditions. To further support this claim, PEIS measurements are taken daily from both HEC/NaCl and E-SGEs sandwiched between stainless steel conductors under ambient conditions. Resulting Nyquist plots are provided in Figure S9c,d (Supporting Information), respectively. It is found that the HEC/NaCl electrolyte became unusable only after 24 h, which is also evident from the drying test provided in Figure S9a (Supporting Information). No significant increase is observed in the impedances of the E-SGEs during the 5 days of the measurements. The series resistance caused by the E-SGE/Stainless steel interface has increased daily, but the increase is minimal. These PEIS measurement results are in agreement with drying tests and prove the water retention ability of E-SGEs.

One fundamental adaptation of nature to flourish in sub-zero conditions is the freeze-tolerance of proteins.[100] It is also proven that proteins effectively inhibit ice recrystallization if they meet the equimolar cation to anion ratio condition.[101] Similarly, zwitterions have shown potential in the fabrication of anti-freezing hydrogels due to the presence of both cations and anions in their structure.[102] Herein, the amino acid content in E-SGEs (with the addition of its zwitterionic form at pH 4.5) shows anti-freezing properties thanks to both mechanisms. In addition to these highly effective zwitterionic protein molecules, the high salt content in soy sauce also helps E-SGE withstand temperatures as cold as −24 °C. Figure S10a,b (Supporting Information) demonstrates the anti-freezing ability of the E-SGEs. Measurements are taken by placing edible supercapacitors into Swagelok cells and placing them in a domestic freezer. It should be noted that long copper cables had to be used to take measurements. Impedance analysis shows that the increase in charge transfer resistance at temperatures below RT, mainly +4 °C and −24 °C, is indeed small and does not preclude the use of supercapacitors. The increase in the series resistance at lower temperatures in the high-frequency region is due to additional cabling for the measurements and the interface between HGC and stainless-steel contacts. Even still, PEIS measurements indicate that the edible supercapacitors still work and can be used in sub-zero conditions. The cyclic voltammograms depicted in Figure S10b (Supporting Information) demonstrate that edible supercapacitors can operate effectively even under an increased IR within the system. Satisfactory performance is achieved with an increased IR even at a high scan rate of 200 mV s^{-1}. The capacitance loss is 32% for +4 °C and 38% for −24 °C. PEIS measurements indicate that the edible supercapacitors perform exceptionally well and are particularly suited for cold environments. The inset photograph in Figure S10b (Supporting Information) shows a photo of an edible supercapacitor kept at −24 °C for 24 h, which is still flexible. This also indicates that the E-SGEs are highly resistant to freezing.

Storage conditions and structural/chemical stability of the edible supercapacitors should also be an essential aspect. Edible energy storage devices, especially those utilizing food-based electrolytes, are mostly susceptible to biodegradation. Thus, they must be kept at freezing temperatures in order to be used on demand.[8,95,97]Therefore, keeping fabricated edible supercapacitors at sub-zero temperatures and then using them in ambient conditions is one way to simulate a real-life use case. For this purpose, a tested edible supercapacitor is kept in the freezer for 1 month and then subjected to electrochemical measurements. Related cyclic voltammograms and PEIS results are provided in Figure S11 (Supporting Information). The drop in capacitance is calculated as 26% from the CV measurements after removal from the freezer (Figure S11a, Supporting Information). At room temperature over time, capacitance retention increased to 76% after 2 h and to 78% after 4 h and remained the same over the course of time. This might be due to interfacial degradation at the electrode/electrolyte interface. Impedance plots (Figure S11b, Supporting Information) show that the interfacial resistance increases after removal from the freezer, which is improved slightly upon keeping at room temperature. The slope at the high frequency region is almost the same as the initial conditions, indicating that the E-SGE retains its fast kinetics. Despite a loss of capacitance, edible supercapacitors can still be used as a reliable energy source. These findings serve as compelling evidence that edible supercapacitors fabricated with E-SGEs hold significant promise for long-term storage and convenient on-demand utilization.

The essence of using food-based electrolytes and biodegradable and compatible components to fabricate edible supercapacitors is to target post-use digestion. **Figure 5**a,b show photographs of the degradation of E-SGEs and a digestion study simulating human gastrointestinal digestion by immersing E-SGE-based edible supercapacitors in gastric fluid. Figure 5a shows the degradation/dissolving of E-SGEs on rocky soil sprinkled with little water daily. After 96 h, it is seen that E-SGEs completely change the color of the rocks and dissolve in the soil, indicating biodegradability. The gastric fluid is prepared according to United States Pharmacopoeia standards for the simulated human gastrointestinal digestion.[103] To imitate gastric peristalsis and the human body's internal environment, the solution temperature is stabilized at 37 °C at a stirring rate of 100 rpm. E-SGE is broken into small pieces in 10 min and completely dissolved in 40 min, giving the color of a mixture of diluted soy sauce and gelatin (Figure S12, Supporting Information). Coupled with the L929 proliferation, it is evident that E-SGEs are highly promising electrolytes for edible energy storage devices. Carbon-based electrodes are also subjected to the digestion study. Within 40 min, electrodes are found to dissolve completely, leaving the suspended carbon particles in the solution (Figure S12, Supporting Information). Moreover, these electrodes, weighing only milligrams, do not pose any harm to the human body.[20] Stemming from these results, edible supercapacitors are also fabricated and subjected to the digestion study, the results of which are provided in Figure 5b. Only after 5 min in gastric fluid the edible supercapacitor begin to decompose. After 20 min, the E-SGE is mostly dissolved, and then within 40 min, the carbon electrodes are found to be completely disintegrated. Therefore, the E-SGE-based edible supercapacitor can be easily digested in just one hour, and this is very promising for the edible electronics field. The edible supercapacitors produced can be used after ingestion according to the needs of digestible health devices, provided they are encapsulated and can be digested when their function is over. Combining these edible supercapacitors, a red LED with a power consumption of ≈140 mW is powered, indicating their high-power output (Figure 5c,d). In summary, edible supercapacitors using E-SGEs as electrolytes and HGC electrodes have the capacity to power small electronic devices and can be safely dissolved or digested after their use is complete.

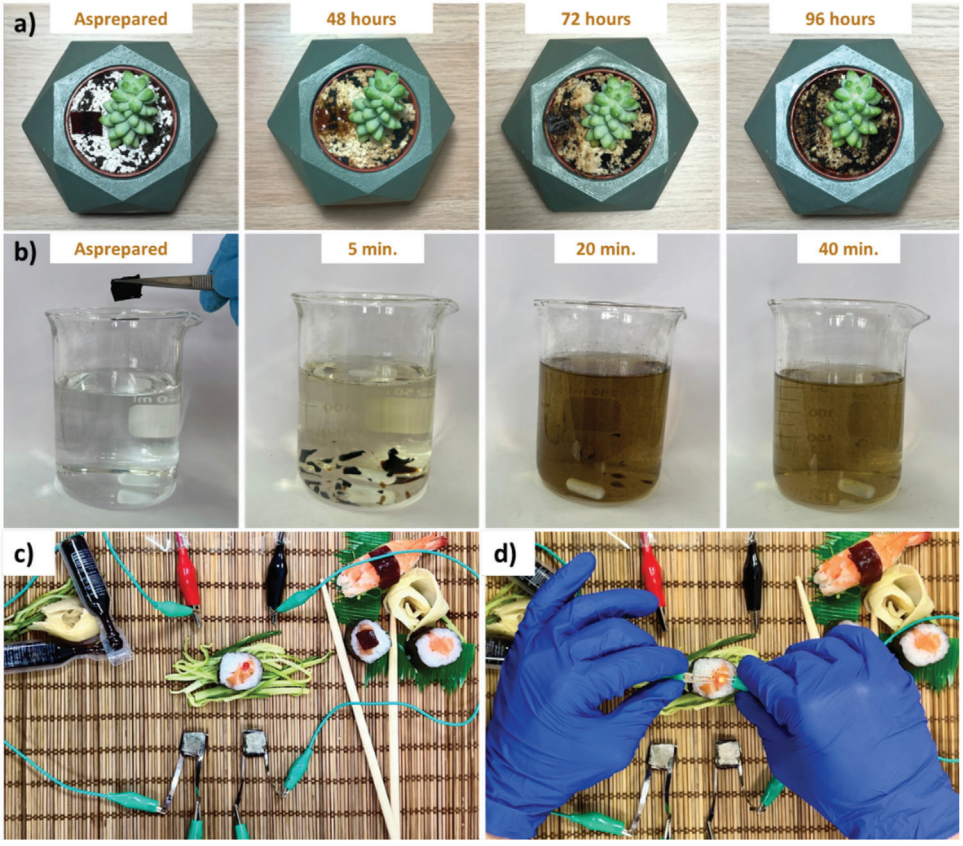

Figure 5. Photographs showing the dissolving of a) E-SGEs on a simple soil that is watered down and b) edible supercapacitors inside the simulated gastric fluid. Photographs of the edible supercapacitors being c) charged and d) used to light an LED with a power consumption of 140 mW.

3. Conclusions

Edible supercapacitors with soy-sauce-based gel electrolytes are demonstrated in this work. The development of this anti-freezing and anti-drying edible gel using a commercial soy sauce provides a very simple way to fabricate electrolytes with superior properties. Developed E-SGEs are shown to have zwitterionic properties, which are proven with zeta potential measurements and detailed FTIR analysis. Moreover, E-SGEs have been shown to allow L929 proliferation – indicating that they are biocompatible and not harmful to cellular growth. E-SGEs fabricated at pH 4.5 are found to be the best-performing electrolyte, and this is further investigated with detailed electrochemical analysis. The edible supercapacitors formed with E-SGEs and HGC electrodes are shown to have textbook-like double-layer capacitance with a maximum specific capacitance of 3.75 F g^{-1} and a capacitance retention of 86.5% after 10 000 cycles. E-SGEs have also shown a substantial resistance to drying and freezing due to the presence of the zwitterionic structure of soy proteins in soy sauce. Degradation studies using a simulated gastric fluid have also shown that all components of the edible supercapacitor can be digested within 40 min. Overall, this research underscores the potential of sustainable and environmentally friendly edible electronics, showcasing their promising prospects in the field. We believe this could serve as a stepping stone in the development of cutting-edge, ingestible healthcare devices and green electronics. With its compelling ionic performance, the edible soy sauce-based electrolyte has the potential to expand the range of alternatives available for traditional energy storage devices.

4. Experimental Section

Materials: Kikkoman Corporation Soy sauce was purchased from a local grocery store. Hydroxyethyl cellulose (HEC) was purchased from Sigma-Aldrich and had a molecular weight of ≈ 90 000. Gelatin was purchased from a local market in the Ankara province. Hydrochloric acid (HCl, ACS reagent, 37%), sodium chloride (NaCl, ACS Reagent), sodium hydroxide (NaOH, ACS Reagent) and vegetable-origin glycerol were also obtained from Sigma-Aldrich. Carbon black (CB, 50% compressed) and activated carbon (AC, −20 +40 mesh) were purchased from Alfa Aesar and used after grinding and sieving, respectively.

Preparation of Edible Soy-Sauce Based Electrolyte (E-SGE) Gels: E-SGE gels were prepared by simple solution mixing and vacuum oven treatment. First, 5 mL of deionized water was added to 5 mL soy sauce. The pH of the solution was adjusted, ranging from 2 to 10. Then, 1.7 gram of HEC and 0.3 grams of gelatin was added to 10 mL of the formed solution. The solution was left stirring on a hot plate at a temperature of 45 °C and stirred at 450 rpm. Then, 0.3 grams of vegetable-origin glycerol was added dropwise. Gelatin was added to increase the water retention ability of the gels. Once the solution became viscous, the pH was rechecked and a shift of ±0.5 was observed relative to the original pH of the solution. The last pH value was accepted as the pH of E-SGE. The shift in pH was due to HEC addition, which has many -OH functional groups. Prepared viscous solutions were

then poured into glass Petri dishes and left in a vacuum oven for 1 hour to obtain E-SGE gels.

Preparation of HEC/Glycerol/CB/AC (HGC) Thin Film Electrodes: HGC electrodes were prepared by solution mixing, followed by doctor blading as described in the previous work.[20] 40 mL of deionized water (DI) was heated until the solution reached 80 °C. Then, 1 gram HEC was added and stirred under 450 rpm. 1.75 grams of ground CB and 0.25 grams of sieved AC were added immediately after the complete dissolution of HEC. Here, HEC also behaved as a surfactant for carbon additives. Later, 1 gram of vegetable-origin glycerol was added. The ink was left string at a solution temperature of 80 °C overnight. After overnight mixture, viscous suspension was doctor bladed with a wet thickness of 500 µm and vacuum dried at 90 °C. The dried HGC can be peeled following vacuum drying to obtain thin film electrodes for supercapacitor devices.

Fabrication of the Edible Zwitterionic SGE Supercapacitor Devices: Flexible HGC-based supercapacitor devices were assembled as follows. E-SGEs and prepared HGC electrodes were punched to a diameter of 11 mm. The average weight of the electrodes was found to be 0.9 mg per electrode. The electrodes were assembled with the E-SGE. The gel state of the E-SGE allowed carbon electrodes to adhere to the surface of the gel, quickly forming a supercapacitor device. Then, the assembled supercapacitor device was used without further processing.

Materials Characterization: SEM characterizations were conducted using FEI NOVA NANO SEM 430 at an operating voltage of 20 kV. Zeta potential measurements were conducted using Malvern ZetaSizer Ultra. Fourier-transform infrared spectroscopy (FTIR) analysis was performed using a Bruker Alpha FTIR spectrometer equipped with an attenuated total reflectance (ATR) unit. The analysis was conducted with a resolution of 4 cm^{-1} within the wavenumber range of 400 – 4000 cm^{-1}. Thermogravimetric Analysis (TGA) was carried out using an Exstar SII TG/DTA 7300 instrument under a nitrogen atmosphere, with a temperature increment of 10°C min^{-1}. The electrical conductivity of the electrodes was measured using 4-point probe technique via Signatone S302.

Biological Characterization of E-SGEs: L929 fibroblasts were used for the biological characterization of the E-SGEs. For these experiments, cells were cultured in a standard culture medium composed of Dulbecco's Modified Eagle's Medium (DMEM) supplemented with 10% fetal bovine serum (FBS), 1% penicillin-streptomycin, and 1% L-glutamine. Prior to the experiments, E-SGE samples were sterilized by UV (30 min for each side) and dissolved in the standard culture media for 72 h to obtain 0.5, 1, 2, and 6 g L^{-1} concentrations. To assess cellular proliferation, fibroblasts were seeded onto culture plates at 10 000 cells per well density in the standard culture media. After 24 h, culture media were replaced with E-SGE dissolved media (standard medium was still used as the control). Fibroblasts were cultured for up to 5 days in vitro under standard cell culture conditions (37°C and 5% CO_2). 3-(4,5-Dimethylthiazol-2-yl)−2,5-diphenyl tetrazolium bromide (MTT) assay was conducted on the 1st, 3rd, and 5th days of culture. Samples were incubated with the MTT reagent for 4 h, followed by aspiration of the MTT solution. 100 µL of 0.1 M HCl solution prepared in isopropanol was applied to each sample to dissolve formazan crystals. The absorbance values of the solutions were read at 570 nm (reference wavelength 670 nm) using a Thermo Scientific Multiskan Go microplate absorbance reader. The absorbance values of blank samples (without any cells) were subtracted from the measured absorbance values. MTT data were normalized so that the control on day 1 corresponded to 100% proliferation. MTT experiments were repeated in triplicate, and three samples were used for each repeat. The data were represented as mean ± standard deviation. Statistical analyses were performed with a one-way analysis of variance using Tukey's post hoc test with significance based on $p < 0.05$.

Fibroblast morphologies were investigated using SEM on the 3rd day of culture. Briefly, cells were fixed with 4% paraformaldehyde solution for 20 min, followed by dehydration successively in 30, 50, 70, 90, and 100% ethanol solutions for 15 min each. Dehydrated cells were treated with hexamethyldisilazane (HMDS, Sigma-Aldrich) and left to dry for 24 h. Samples were coated with gold–palladium prior to SEM imaging. Cellular morphologies of the adherent fibroblasts were also investigated with confocal microscopy on the 3rd day of culture. For these experiments, cells were fixed with 4% paraformaldehyde for 20 min. Cellular membranes were permeated with 0.1% Triton X-100 for 30 min. F-actin filaments were stained with rhodamine-phalloidin for 20 min, and nuclei were stained with DAPI (1:40000) for 30 min. Confocal microscopy (Zeiss LSM800) was used for imaging. Captured images were merged with ZEISS ZEN Imaging Software. To measure cellular spreading, 50 cells from different confocal images were analyzed for each sample using ImageJ software.

Electrochemical Measurements: Biologic VMP3 galvanostat/potentiostat was used for electrochemical characterization. A symmetric 2-electrode setup with a Swagelok cell was used for the electrochemical measurements. The HGC electrodes acted as anode and cathode, and the edible zwitterionic E-SGE acted as both electrolyte and separator. Since the device performs best in the voltage range of 0 to 1 V, the cyclic voltammetry (CV) and galvanostatic charge/discharge (GCD) measurements were done at different scan rates and current densities. EIS measurements were conducted within a frequency range of 200 kHz – 50 mHz, employing a sinusoidal AC amplitude of 10 mV at an open circuit voltage (E_{oc}). The cycling performance of the fabricated edible supercapacitors was determined after 10 000 cycles at a scan rate of 200 mV s^{-1}.

Electrochemical characterization in the cold environment (refrigerator) was done using a portable Gamry 3000 Reference galvanostat/potentiostat. All analyses were performed with the same parameters as above.

The specific capacitance of the (C_{sp}) was measured from CV analysis using the equation:

$$C_{Sp} = \int_{Ei}^{Ef} idV / 2Evm \tag{1}$$

where E is the voltage range (V), ν is the scan rate (mV s^{-1}), m is the total mass of the electrodes (g), and i is the current (mA).

Ionic conductivity of the E-SGE was calculated from the impedance measurements with stainless steel contacts using the equation below;

$$\delta = \frac{1}{R_b}\frac{d}{S} \tag{2}$$

where δ is the ionic conductivity (S cm^{-1}), R_b is the bulk resistance obtained from the real impedance end of the semicircular area at high-frequency region (Ω), d is the thickness of the E-SGE (cm), and S is the contact area of the E-SGEs.

Energy (W h kg^{-1}) density (E) and power (W kg^{-1}) density (P) values were calculated using the GCD curves and the equations below

$$E = \frac{1}{2} C V^2 \tag{3}$$

$$P = \frac{E}{\Delta t} \tag{4}$$

where C is the capacitance value calculated from GCD, V is the voltage range, and Δt is the discharge time (h).

Preparation of Zeta Potential Measurement Samples of E-SGEs: Zeta potential measurements were conducted using Malvern ZetaSizer Ultra. 1 mL of soy sauce was dispersed in 100 mL of de-ionized water in the ultrasonic bath for 15 min. The monomodal mode was selected during the zeta potential measurements to minimize the sample delicacy during the electric field application. pH adjustments were made with the addition of 0.1 M HCl and 0.1 M NaOH.

Preparation of Simulated Gastric Fluid and Dissolving of E-SGE-Based Edible Supercapacitors: The simulated gastric fluid (SGF) was prepared according to the United States Pharmacopoeia standards. SGF was ready by 0.03 M NaCl solution adjusted at pH 1.2 with 1 M of HCl solution with 3.2 mg mL^{-1} pepsin enzyme. To imitate gastric peristalsis and the human body's internal environment, the hot plate speed was adjusted to 100 rpm, and the solution temperature was stabilized at 37 °C.

Supporting Information

Supporting Information is available from the Wiley Online Library or from the author.

Acknowledgements

The authors would like to thank Nanovatif Materials Technologies for the use of instrumentation and infrastructure. The authors also thank Ozan Berk Boyraz, Loay Madbouly, and Moustafa Saada for their support of illustrations.

Conflict of Interest

The authors declare no conflict of interest.

Author Contributions

M.B.D. and D.K. contributed equally to this work. H.E.U. proposed the project. H.E.U., M.B.D., D.K, and M.O. C. conceived the idea. D. K. performed the fabrication of components. M.B.D. and D.K. performed characterizations, electrochemical measurements, data analysis, and its interpretation. O.D. performed zeta potential measurements, data analysis, and interpretation. Y.T. performed biological characterizations, data analysis, and its interpretation. B.Y. performed rheology measurements. M.B.D. and D.K. organized and wrote the manuscript. S.C.A. and B.E. contributed to discussions and reviewing of the manuscript. H.E.U. performed supervision, writing-reviewing, and editing the manuscript.

Data Availability Statement

The data that support the findings of this study are available from the corresponding author upon reasonable request.

Keywords

edible, gel electrolytes, supercapacitors, zwitterionic

Received: June 21, 2023
Revised: September 15, 2023
Published online:

[1] C. J. Bettinger, *Trends Biotechnol.* **2015**, *33*, 575.
[2] L. Lamanna, P. Cataldi, M. Friuli, C. Demitri, M. Caironi, *Adv. Mater. Technol.* **2022**, *8*, 2200731.
[3] H. Sheng, X. Zhang, J. Liang, M. Shao, E. Xie, C. Yu, W. Lan, *Adv. Healthcare Mater.* **2021**, *10*, 2100199.
[4] P. Cataldi, L. Lamanna, C. Bertei, F. Arena, P. Rossi, M. Liu, F. Di Fonzo, D. G. Papageorgiou, A. Luzio, M. Caironi, *Adv. Funct. Mater.* **2022**, *32*, 2113417.
[5] A. G. Keller, A. Gregory, *Smart Materials for Edible Devices Smart Materials for Edible Devices Recommended Citation Recommended Citation*, **2020**.
[6] A. Keller, J. Pham, H. Warren, M. In het Panhuis, *J. Mater. Chem. B* **2017**, *5*, 5318.
[7] X. Wang, W. Xu, P. Chatterjee, C. Lv, J. Popovich, Z. Song, L. Dai, M. Y. S. Kalani, S. E. Haydel, H. Jiang, *Adv. Mater. Technol.* **2016**, *1*, 1600059.
[8] W. Xu, H. Yang, W. Zeng, T. Houghton, X. Wang, R. Murthy, H. Kim, Y. Lin, M. Mignolet, H. Duan, H. Yu, M. Slepian, H. Jiang, *Adv. Mater. Technol.* **2017**, *2*, 1700181.
[9] I. K. Ilic, V. Galli, L. Lamanna, P. Cataldi, L. Pasquale, V. F. Annese, A. Athanassiou, M. Caironi, *Adv. Mater.* **2023**, *35*, 2211400.
[10] A. S. Sharova, M. Caironi, *Adv. Mater.* **2021**, *33*, 2103183.
[11] R. Kautz, D. D. Ordinario, V. Tyagi, P. Patel, T. N. Nguyen, A. A. Gorodetsky, *Adv. Mater.* **2018**, *30*, 1704917.
[12] H. Hafezi, T. L. Robertson, G. D. Moon, K.-Y. Au-Yeung, M. J. Zdeblick, G. M. Savage, *IEEE Trans. Biomed. Eng.* **2015**, *62*, 99.
[13] W. Li, Q. Liu, Y. Zhang, C. Li, Z. He, W. C. H. Choy, P. J. Low, P. Sonar, A. K. K. Kyaw, *Adv. Mater.* **2020**, *32*, 2001591.
[14] A. S. Sharova, F. Melloni, G. Lanzani, C. J. Bettinger, M. Caironi, *Adv. Mater. Technol.* **2021**, *6*, 2000757.
[15] Y. Su, N. Li, L. Wang, R. Lin, Y. Zheng, G. Rong, M. Sawan, *Adv. Mater. Technol.* **2022**, *7*, 2100608.
[16] X. Tong, G. Sheng, D. Yang, S. Li, C.-W. Lin, W. Zhang, Z. Chen, C. Wei, X. Yang, F. Shen, Y. Shao, H. Wei, Y. Zhu, J. Sun, R. B. Kaner, Y. Shao, *Mater. Horiz.* **2022**, *9*, 383.
[17] Y. Liu, H. Zhou, W. Zhou, S.i Meng, C. Qi, Z. Liu, T. Kong, *Adv. Energy Mater.* **2021**, *11*, 2101329.
[18] A. Rafieerad, A. Amiri, G. L. Sequiera, W. Yan, Y. Chen, A. A. Polycarpou, S. Dhingra, *Adv. Funct. Mater.* **2021**, *31*, 2100015.
[19] D. Ohayon, S. Inal, *Adv. Mater.* **2020**, *32*, 2001439.
[20] M. B. Durukan, M. O. Cicek, D. Doganay, M. C. Gorur, S. Cinar, H. E. Unalan, *Adv. Funct. Mater.* **2022**, *32*, 2106066.
[21] X.u Wang, W. Xu, P. Chatterjee, C. Lv, J. Popovich, Z. Song, L. Dai, M. Y. S. Kalani, S. E. Haydel, H. Jiang, *Adv. Mater. Technol.* **2016**, *1*, 1600059.
[22] K. Chen, L. Yan, Y. Sheng, Y. Ma, L. Qu, Y. Zhao, *ACS Nano* **2022**, *16*, 15261.
[23] X. Jia, C. Wang, C.-Y. Lee, C. Yu, G. G. Wallace, *MRS Bull.* **2020**, *45*, 121.
[24] G. Lee, S. K. Kang, S. M. Won, P. Gutruf, Y. R. Jeong, J. Koo, S. S. Lee, J. A. Rogers, J. S. Ha, *Adv. Energy Mater.* **2017**, *7*, 1700157.
[25] X. Huang, D. Wang, Z. Yuan, W. Xie, Y. Wu, R. Li, Y. Zhao, D. Luo, L. Cen, B. Chen, H. Wu, H. Xu, X. Sheng, M. Zhang, L. Zhao, L. Yin, *Small* **2018**, *14*, 1800994.
[26] X. Aeby, A. Poulin, G. Siqueira, M. K. Hausmann, G. Nyström, *Adv. Mater.* **2021**, *33*, 2101328.
[27] H. F. Smyth, C. P. Carpenter, C. S. Weil, *Journal of the American Pharmaceutical Association* **1947**, *36*, 335.
[28] T. Jiang, W. Tang, X. Chen, C. Bao Han, L. Lin, Y. Zi, Z. L. Wang, *Adv. Mater. Technol.* **2016**, *1*, 1600059.
[29] C. Gao, C. Bai, J. Gao, Y. Xiao, Y. Han, A. Shaista, Y. Zhao, L. Qu, *J Mater Chem A Mater* **2020**, *8*, 4055.
[30] R. Wang, M. Yao, S. Huang, J. Tian, Z. Niu, *Adv. Funct. Mater.* **2021**, *31*, 2009209.
[31] G. Lee, S.-K. Kang, S. M. Won, P. Gutruf, Y. R. Jeong, J. Koo, S.-S. Lee, J. A. Rogers, J. S. Ha, *Adv. Energy Mater.* **2017**, *7*, 1700157.
[32] Xun, Ni, Gao, Zhang, Gu, Huo, *Polymers (Basel)* **2019**, *11*, 1895.
[33] P. Huo, S. Ni, P.u Hou, Z. Xun, Y. Liu, J. Gu, *Polymers (Basel)* **2019**, *11*, 863.
[34] J. Wang, Z. Xun, C. Zhao, Y. Liu, J. Gu, P. Huo, *Int. J. Biol. Macromol.* **2022**, *209*, 268.
[35] M. Zhu, C. Tan, Q. Fang, L. Gao, G. Sui, X. Yang, *ACS Sustain Chem Eng* **2016**, *4*, 4498.
[36] X. Peng, H. Liu, Q. Yin, J. Wu, P. Chen, G. Zhang, G. Liu, C. Wu, Y. Xie, *Nat. Commun.* **2016**, *7*, 11782.
[37] K. Fang, R. Wang, H. Zhang, L. Zhou, T. Xu, Y. Xiao, Y. Zhou, G. Gao, J. Chen, D. Liu, F. Ai, J. Fu, *ACS Appl. Mater. Interfaces* **2020**, *12*, 52307.
[38] C. Tiyapiboonchaiya, J. M. Pringle, J. Sun, N. Byrne, P. C. Howlett, D. R. MacFarlane, M. Forsyth, *Nat. Mater.* **2004**, *3*, 29.

[39] X. Peng, H. Liu, Q. Yin, J. Wu, P. Chen, G. Zhang, G. Liu, C. Wu, Y. Xie, *Nat. Commun.* **2016**, *7*, 11782.
[40] F. Mo, Z.e Chen, G. Liang, D. Wang, Y. Zhao, H. Li, B. Dong, C. Zhi, *Adv. Energy Mater.* **2020**, *10*, 2000035.
[41] C. Liu, F. Li, G. Li, P. Li, A. Hu, Z. Cui, Z. Cong, J. Niu, *ACS Appl. Mater. Interfaces* **2022**, *14*, 9608.
[42] B. Zhang, E. Ryan, X. Wang, W. Song, S. Lindsay, *ACS Nano* **2022**, *16*, 1671.
[43] S. Lindsay, *Life* **2020**, *10*, 72.
[44] J. Nan, G. Zhang, T. Zhu, Z. Wang, L. Wang, H. Wang, F. Chu, C. Wang, C. Tang, *Adv. Sci.* **2020**, *7*, 2000587.
[45] Xun, Ni, Gao, Zhang, Gu, Huo, *Polymers (Basel)* **2019**, 1895, *11*,.
[46] F. Chen, X. Wang, M. Armand, M. Forsyth, *Nat. Mater.* **2022**, *21*, 1175.
[47] Y. Zhao, Y. Bai, Y. Bai, M. An, G. Chen, W. Li, C. Li, Y. Zhou, *J. Power Sources* **2018**, *407*, 23.
[48] M. A. S. Azha, E. M. A. Dannoun, S. B. Aziz, M. F. Z. Kadir, Z. I. Zaki, Z. M. El-Bahy, M. Sulaiman, M. M. Nofal, *Polymers (Basel)* **2021**, *13*, 3602.
[49] Y. Zhao, M. He, L. Zhao, S. Wang, Y. Li, L. Gan, M. Li, L. Xu, P. R. Chang, D. P. Anderson, Y. Chen, *ACS Appl. Mater. Interfaces* **2016**, *8*, 2781.
[50] V. Selvanathan, M. N. A. Halim, A. D. Azzahari, M. Rizwan, N. Shahabudin, R. Yahya, *Ionics (Kiel)* **2018**, *24*, 1955.
[51] M. Y. Chong, A. Numan, C.-W. Liew, K. Ramesh, S. Ramesh, *J. Appl. Polym. Sci.* **2017**, *134*, 44636.
[52] S. Gupta, P. K. Varshney, *Ionics (Kiel)* **2017**, *23*, 1613.
[53] Y. N. Sudhakar, M. Selvakumar, D. K. Bhat, *Mater Renew Sustain Energy* **2015**, *4*, 10.
[54] M. Y. Zhang, M. X. Li, Z. Chang, Y. F. Wang, J. Gao, Y. S. Zhu, Y. P. Wu, W. Huang, W. Huang, *Electrochim. Acta* **2017**, *245*, 752.
[55] X. Ma, X. Zuo, J. Wu, X. Deng, X. Xiao, J. Liu, J. Nan, *J Mater Chem A Mater* **2018**, *6*, 1496.
[56] D. Zhao, Y. Zhu, W. Cheng, W. Chen, Y. Wu, H. Yu, *Adv. Mater.* **2021**, *33*, 2000619.
[57] S. M. F. Kabir, P. P. Sikdar, B. Haque, M. A. R. Bhuiyan, A. Ali, M. N. Islam, *Prog Biomater* **2018**, *7*, 153.
[58] Y. Zhao, M. He, L. Zhao, S. Wang, Y. Li, L. Gan, M. Li, L. Xu, P. R. Chang, D. P. Anderson, Y. Chen, *ACS Appl. Mater. Interfaces* **2016**, *8*, 2781.
[59] M. Chen, J. Chen, W. Zhou, X. Han, Y. Yao, C.-P. Wong, *Adv. Mater.* **2021**, *33*, 2007559.
[60] J. Song, S. Chen, L. Sun, Y. Guo, L. Zhang, S. Wang, H. Xuan, Q. Guan, Z. You, *Adv. Mater.* **2020**, *32*, 1906994.
[61] X. Sui, H. Guo, C. Cai, Q. Li, C. Wen, X. Zhang, X. Wang, J. Yang, L. Zhang, *Chem. Eng. J.* **2021**, *419*, 129478.
[62] S. Xue, Y. Wu, M. Guo, Y. Xia, D. Liu, H. Zhou, W. Lei, *Soft Matter* **2019**, *15*, 3680.
[63] E. Miranda-Bermudez, N. Belai, B. P. Harp, B. J. Yakes, J. N. Barrows, *Food Additives & Contaminants: Part A* **2012**, *29*, 38.
[64] Y. Chyan, R. Ye, Y. Li, S. P. Singh, C. J. Arnusch, J. M. Tour, *ACS Nano* **2018**, *12*, 2176.
[65] D. Fukushima, *J. Am. Oil Chem. Soc.* **1981**, *58*, 346.
[66] B. Yang, H. Yang, J. Li, Z. Li, Y. Jiang, *Food Chem.* **2011**, *124*, 551.
[67] R. Wang, M. Yao, S. Huang, J. Tian, Z. Niu, *Adv. Funct. Mater.* **2021**, *31*, 2009209.
[68] C. Diez-Simon, C. Eichelsheim, D. M. Jacobs, R. Mumm, R. D. Hall, *Food Research International* **2021**, *144*, 110348.
[69] C. Diez-Simon, C. Eichelsheim, R. Mumm, R. D. Hall, *J. Agric. Food Chem.* **2020**, *68*, 11612.
[70] M. Wang, S. Kuang, X. Wang, D. Kang, D. Mao, G. Qian, X. Cai, M. Tan, F. Liu, Y. Zhang, *Membranes (Basel)* **2021**, *11*, 408.
[71] K. M. Goh, O. M. Lai, F. Abas, C. P. Tan, *Food Chem.* **2017**, *215*, 200.
[72] B. M. Broome, M. H. Hecht, *J. Mol. Biol.* **2000**, *296*, 961.
[73] S. Azari, L. Zou, *J Memb Sci* **2012**, *401–402*, 68.
[74] A. Malhotra, J. N. Coupland, *Food Hydrocoll* **2004**, *18*, 101.
[75] A. M. Alswieleh, N. Cheng, I. Canton, B. Ustbas, X. Xue, V. Ladmiral, S. Xia, R. E. Ducker, O. El Zubir, M. L. Cartron, C. N. Hunter, G. J. Leggett, S. P. Armes, *J. Am. Chem. Soc.* **2014**, *136*, 9404.
[76] Z. Wang, L. Zhang, X. Zhang, M. Zeng, Z. He, J. Chen, *Food Biophys* **2021**, *16*, 484.
[77] D. P. Jaramillo, R. F. Roberts, J. N. Coupland, *Food Research International* **2011**, *44*, 911.
[78] M. Lam, R. Shen, P. Paulsen, M. Corredig, *Food Research International* **2007**, *40*, 101.
[79] M. L. F. Freitas, K. M. Albano, V. R. N. Telis, *Polímeros* **2017**, *27*, 62.
[80] L. Deng, Z. Wang, S. Yang, J. Song, F. Que, H. Zhang, F. Feng, *PLoS One* **2016**, *11*, e0160101.
[81] R. Wang, M. Yao, S. Huang, J. Tian, Z. Niu, *Adv. Funct. Mater.* **2021**, *31*, 2009209.
[82] N. Reddy, Z. Shi, H. Xu, Y. Yang, *J Biomed Mater Res A* **2015**, *103*, 1653.
[83] L. Wang, Z. Yin, J. Wu, Z. Sun, B. Xie, *J. Food Eng.* **2008**, *88*, 186.
[84] G. Stojkov, Z. Niyazov, F. Picchioni, R. K. Bose, *Gels* **2021**, *7*, 255.
[85] S. Sathaye, A. Mbi, C. Sonmez, Y. Chen, D. L. Blair, J. P. Schneider, D. J. Pochan, *Wiley Interdiscip Rev Nanomed Nanobiotechnol* **2015**, *7*, 34.
[86] B. Z. Chowdhry, T. J. Dines, S. Jabeen, R. Withnall, *J. Phys. Chem. A* **2008**, *112*, 10333.
[87] M. N. Blom, I. Compagnon, N. C. Polfer, G. Von Helden, G. Meijer, S. Suhai, B. Paizs, J. Oomens, *J. Phys. Chem. A* **2007**, *111*, 7309.
[88] N. Varshney, A. K. Sahi, S. Poddar, N. K. Vishwakarma, G. Kavimandan, A. Prakash, S. K. Mahto, *ACS Appl. Mater. Interfaces* **2022**, *14*, 14033.
[89] S. Tansaz, A. R. Boccaccini, *J Biomed Mater Res A* **2016**, *104*, 553.
[90] Y. Tokudome, K. Nakamura, M. Kage, H. Todo, K. Sugibayashi, F. Hashimoto, *Int J Food Sci Nutr* **2012**, *63*, 689.
[91] S. Ahn, C. O. Chantre, A. R. Gannon, J. U. Lind, P. H. Campbell, T. Grevesse, B. B. O'connor, K. K. Parker, *Adv. Healthcare Mater.* **2018**, *7*, 1701175.
[92] A. Leask, *Adv Wound Care* **2013**, *2*, 160.
[93] M.-Y. Han, H. Kosako, T. Watanabe, S. Hattori, *Mol. Cell. Biol.* **2007**, *27*, 8190.
[94] A. J. Gupta, H. Gruppen, D. Maes, J.-W. Boots, P. A. Wierenga, *J. Agric. Food Chem.* **2013**, *61*, 10613.
[95] S. Alesaeidi, M. S. Kahrizi, A. Ghorbani Tajani, H. Hajipour, M. Ghorbani, *J. Polym. Environ.* **2023**, *31*, 396.
[96] A. Lasia, *J. Phys. Chem. Lett.* **2022**, *13*, 580.
[97] R. Wang, M. Yao, S. Huang, J. Tian, Z. Niu, *Adv. Funct. Mater.* **2021**, *31*, 2009209.
[98] C. Lu, X.i Chen, *Nano Lett.* **2020**, *20*, 1907.
[99] X. Su, H. Wang, Z. Tian, X. Duan, Z. Chai, Y. Feng, Y. Wang, Y. Fan, J. Huang, *ACS Appl. Mater. Interfaces* **2020**, *12*, 29757.
[100] C. I. Biggs, T. L. Bailey, Ben Graham, C. Stubbs, A. Fayter, M. I. Gibson, *Nat. Commun.* **2017**, *8*, 1546.
[101] D. E. Mitchell, N. R. Cameron, M. I. Gibson, *Chem. Commun.* **2015**, *51*, 12977.
[102] J. Yang, Z. Xu, J. Wang, L. Gai, X. Ji, H. Jiang, L. Liu, *Adv. Funct. Mater.* **2021**, *31*, 2009438.
[103] T.-J. Fu, U. R. Abbott, C. Hatzos, *J. Agric. Food Chem.* **2002**, *50*, 7154.